

Tetrahedral mesh improvement via optimization of the element condition number

Lori A. Freitag^{1,*} and Patrick M. Knupp²

¹ *Computer Scientist, Mathematics and Computer Science Division, Argonne National Laboratory, Argonne, IL 60439. freitag@mcs.anl.gov.*

² *Member of Technical Staff, Parallel Computing Sciences Department, Sandia National Laboratories, M/S 0441, P.O. Box 5800, Albuquerque, NM 87185-0441. pknupp@sandia.gov*

SUMMARY

We present a new shape measure for tetrahedral elements that is optimal in that it gives the distance of a tetrahedron from the set of inverted elements. This measure is constructed from the condition number of the linear transformation between a unit equilateral tetrahedron and any tetrahedron with positive volume. Using this shape measure, we formulate two optimization objective functions that are differentiated by their goal: the first seeks to improve the average quality of the tetrahedral mesh; the second aims to improve the worst-quality element in the mesh. We review the optimization techniques used with each objective function and present experimental results that demonstrate the effectiveness of the mesh improvement methods. We show that a combined optimization approach that uses both objective functions obtains the best-quality meshes for several complex geometries.

KEY WORDS: Mesh Improvement, Optimization-based Mesh Smoothing, Mesh Quality, Element Condition Number

1. Introduction

Local mesh smoothing algorithms are commonly used for simplicial mesh improvement. These methods relocate a set of adjustable vertices, one at a time, to improve mesh quality in a neighborhood of that vertex. The new grid point position is determined by considering a local submesh containing the adjustable, or *free*, vertex, v , and its incident vertices and elements. Overall

*Correspondence to: Mathematics and Computer Science Division, Argonne National Laboratory, Argonne, IL 60439.

Contract/grant sponsor: The work of the first author was supported by the Mathematical, Information, and Computational Sciences Division subprogram of the Office of Advanced Scientific Computing Research, U.S. Department of Energy, under Contract W-31-109-Eng-38. The work of the second author was supported by the Department of Energy's Mathematics, Information and Computational Sciences Program (SC-31) and was performed at Sandia National Laboratories. Sandia is a multiprogram laboratory operated by Sandia Corporation, a Lockheed Martin Company, for the United States Department of Energy under Contract DE-ACO4-94AL85000.

improvement in the mesh is obtained by performing some number of sweeps over the set of adjustable vertices.

The most commonly used local mesh smoothing technique is Laplacian smoothing[7, 20] which moves the free vertex to the geometric center of its incident vertices. Laplacian smoothing is computationally inexpensive but does not guarantee improvement in element quality. To address this problem, several optimization-based approaches to mesh smoothing have been developed in recent years.[23, 13, 1, 22, 16] In these techniques, the local submesh is evaluated according to some objective function based on a quality metric such as element angle or aspect ratio. Function and, possibly, gradient information are used to relocate the free vertex in such a way that the objective function is optimized.

Several optimization objective functions based on geometric criteria have been proposed for *a priori* improvement of a simplicial mesh. For example, Bank proposed a ratio of triangle area to edge length squared for two-dimensional meshes,[2] Shephard and Georges proposed a similar ratio of volume to face areas for tetrahedral meshes,[23] Freitag et. al. used angle-based measures for both two- and three-dimensional meshes,[11, 13] and Knupp has proposed a number of shape quality measures derived from simplicial element Jacobian matrices.[16, 15] Canann et. al. proposed a distortion metric for both triangles and quadrilaterals that could be used with both valid and inverted elements.[22] In addition, *a posteriori* metrics have been proposed by Bank and Smith to improve finite element meshes by optimizing solution error indicators.[1]

In Section 2, we propose a new quality metric for the *a priori* improvement of tetrahedral meshes. The metric is based on the condition number of the linear transformation from an equilateral tetrahedron to an arbitrary tetrahedron. We show that the condition number metric is a tetrahedral shape measure according to the formal definition given in Dompierre, et. al.[5] and that it is optimal in that it gives the distance of a tetrahedron to the set of inverted elements. We show that this previously overlooked metric is well-motivated, no more expensive to compute than other commonly-used shape measures, and effective. In addition, the condition number metric is notable because it is referenced to the “ideal” element. This allows us to flexibly choose our ideal element shape and thereby reference element quality to an ideal anisotropic element as well as to an isotropic one. We have proved that the metric is equivalent (in the sense of Liu and Joe[19]) to the Mean Ratio metric.[21, 17]

In Section 3, we formulate two optimization objective functions using the element condition number that are suitable for mesh improvement if the initial mesh is valid. The first objective function targets the improvement of average element quality; the second targets the improvement of the worst element quality. In previous papers, we have independently proposed optimization techniques for mesh improvement as measured by average element quality[16] and mesh improvement as measured by extremal element quality,[13] and we review these optimization techniques in Section 3.2. If the initial mesh is not valid, it may be preprocessed using an optimization-based mesh untangling approach that creates valid, although poor-quality, elements.[10, 12, 18]

In Section 4, we present numerical results for each optimization approach on four tetrahedral meshes. We compare each technique to a baseline Laplacian smoother, and illustrate that in all test cases, a combined optimization approach produces the best-quality meshes. Finally, in Section 5, we offer concluding remarks and directions for future research.

2. Tetrahedral Jacobian Matrices and Condition Numbers

To facilitate our discussion of the condition number quality metric, we first discuss the linear transformations associated with triangular and tetrahedral elements. Figure 1 illustrates the two-dimensional case. Let t be an arbitrary triangular element consisting of three vertices v_n , $n = 0, 1, 2$, with coordinates $\mathbf{x}_n \in R^3$. Define the edge vectors

$$e_{k,n} = \mathbf{x}_k - \mathbf{x}_n \quad (1)$$

with $k \neq n$ and $k = 0, 1, 2$. Vertex v_n has two attached edge vectors, $e_{n+1,n}$ and $e_{n+2,n}$, where the indices are taken modulo three. The columns of the Jacobian matrix, denoted A , consist of the edge vectors attached to a vertex. This linear transformation takes points in the reference triangle (a right-angled triangle) to points in the physical triangle, t . Define the matrix W such that it transforms the reference triangle to an ideal, equilateral triangle. Then the matrix $S = AW^{-1}$ transforms the ideal triangle to the physical triangle. This linear transformation is critical because it measures the deviation of the physical triangle from the ideal shape.

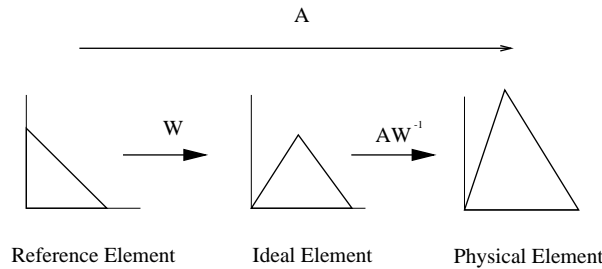


Figure 1. The relationship between the linear transformations and the reference, ideal, and physical elements

A critical part of the theory to be presented are the matrix norms associated with these linear transformations, and we briefly review that information now. Let I be the identity matrix, and S be an arbitrary matrix. The Frobenius norm of S is defined in terms of the trace:

$$|S| = [tr(S^T S)]^{1/2}.$$

The Frobenius norm is invariant to rotation matrices, that is, $|SR| = |RS| = |S|$, where R is a rotation matrix ($R^T R = I$, $det(R) = 1$). If S is invertible, then S^{-1} exists, and one can define the adjoint matrix of S :

$$adj(S) = det(S) S^{-1}.$$

Similarly, matrices and linear transformations can be defined for tetrahedral elements, and we now construct a new tetrahedral shape measure based on the resulting norms and matrix condition number.

2.1. Tetrahedral Jacobian Matrices

For the three dimensional case, let T be an arbitrary tetrahedral element consisting of four vertices v_n , $n = 0, 1, 2, 3$ with coordinates $\mathbf{x}_n \in R^3$. Define the edge vectors, $e_{k,n}$, as in Equation 1 for

$k = 0, 1, 2, 3$ and note that $e_{n,k} = -e_{k,n}$. Each vertex v_n of the tetrahedra has three attached edge vectors, $e_{n+1,n}$, $e_{n+2,n}$, and $e_{n+3,n}$, where the indices are taken modulo four. In this case the Jacobian matrix at node n , denoted A_n , consists of the columns of the triplet of attached edge vectors, namely,

$$A_n = (-1)^n \begin{pmatrix} e_{n+1,n} & e_{n+2,n} & e_{n+3,n} \end{pmatrix}.$$

Let α_n be the determinant of A_n . A right-handed rule is assumed for the edge-ordering so that $\alpha_n > 0$ for elements with positive volume. Let $\mathcal{V}(T)$ denote the volume of the tetrahedron.

Theorem 1. The determinants of A_n are independent of n ; that is $\alpha_n = \alpha_0$ for $n = 1, 2, 3$.

Proof.

Let M be the following constant matrix

$$M = \begin{pmatrix} 1 & 1 & 1 \\ -1 & 0 & 0 \\ 0 & -1 & 0 \end{pmatrix}.$$

The determinant of M equals 1. A direct calculation shows that

$$A_n = A_0 M^n$$

for $n = 1, 2, 3$. Taking the determinant of this expression gives $\alpha_n = \alpha_0$. §

It is well known that the volume of a tetrahedron is one-sixth of the Jacobian determinant,[14] hence $\alpha_0 = 6 \mathcal{V}(T)$ and $\mathcal{V}(T) > 0$ if and only if $\alpha_0 > 0$. An element is said to be *valid* if and only if $\alpha_0 > 0$.

One can easily show that the following relationships hold for the Jacobian matrix:

$$|A_n|^2 = |e_{n+1,n}|^2 + |e_{n+2,n}|^2 + |e_{n+3,n}|^2, \quad \text{and}$$

$$|\text{adj}(A_n)|^2 = |e_{n+1,n} \times e_{n+2,n}|^2 + |e_{n+2,n} \times e_{n+3,n}|^2 + |e_{n+3,n} \times e_{n+1,n}|^2,$$

which provide a geometric interpretation of the norms. The norm-squared of A_n is the sum of the lengths-squared of the attached edge vectors and the norm-squared of the adjoint is the sum of the squares of the areas of the attached triangular faces.

Unlike the determinant α_n , the norms of A_n and $\text{adj}(A_n)$ are not independent of n because not all of the lengths and areas of the tetrahedron affect the result for A_n . However, one can create a weighted Jacobian matrix that is independent of n , as will be shown next.

Define an equilateral tetrahedron T_e to have sides of length one and four vertices with the coordinates $(0, 0, 0)$, $(1, 0, 0)$, $(1/2, \sqrt{3}/2, 0)$, and $(1/2, \sqrt{3}/6, \sqrt{2}/\sqrt{3})$. This tetrahedron serves as the ideal element. Let W_n be the Jacobian matrix at the n th vertex of T_e . For example,

$$W_0 = \begin{pmatrix} 1 & 1/2 & 1/2 \\ 0 & \sqrt{3}/2 & \sqrt{3}/6 \\ 0 & 0 & \sqrt{2}/\sqrt{3} \end{pmatrix}$$

and $w_0 = \det(W_0) = \sqrt{2}/2$.

Theorem 2.

Let T be any tetrahedron with Jacobian matrices A_n and S_n be the linear transformation that takes W_n to A_n , then $S_n = A_0 W_0^{-1}$. That is, S_n is independent of n .

Proof.

By definition, $S_n W_n = A_n$. If $n = 0$, $S_0 = A_0 W_0^{-1}$. Theorem 1 applies to the matrices W_n of T_e . Thus $W_n = W_0 M^n$ for $n = 1, 2, 3$. Because $A_n = A_0 M^n$, we have the stated result. §

In other words, there exists a unique linear transformation between the ideal tetrahedron T_e and the physical tetrahedron T . Thus, let us denote W_0 by W and w_0 by w .

Theorem 3.

The norms $|A_n W^{-1}|$ and $|W A_n^{-1}|$ are independent of n . That is $|A_n W^{-1}| = |A_0 W^{-1}|$ and $|W A_n^{-1}| = |W A_0^{-1}|$.

Proof.

The result for $n = 0$ is immediate. Define the matrix $R = W M W^{-1}$, where M is defined in the proof of Theorem 1. A direct calculation shows that R is a rotation matrix with a positive determinant. Therefore, $\det(R^n) = 1$ and $(R^n)^T R^n = I$ for $n = 1, 2, 3$. Hence

$$\begin{aligned} |A_n W^{-1}| &= |A_0 M^n W^{-1}| \\ &= |A_0 W^{-1} R^n| \\ &= |A_0 W^{-1}|. \end{aligned}$$

Similarly, the second result can be proved by observing that $W A_n^{-1} = (A_n W^{-1})^{-1} = (R^n)^{-1} W A_0^{-1}$ and showing that $(R^n)^{-1}$ is a rotation matrix. §

2.2. Tetrahedral Condition Numbers

Let T_+ be any valid tetrahedron. Then A_n^{-1} exists, and one can compute the weighted *condition number* of the matrix A_n

$$\kappa_w(A_n) = |A_n W^{-1}| | (A_n W^{-1})^{-1} |.$$

Because $(A_n W^{-1})^{-1} = W A_n^{-1}$, Theorem 3 shows that $\kappa_w(A_n)$ is independent of n which is not true for the unweighted condition number $\kappa(A_n) = |A_n| |A_n^{-1}|$. Now let A be any of the four Jacobian matrices of T_+ and $\kappa_w(A) = |A W^{-1}| |W A^{-1}|$. Recall that $S = A W^{-1}$ is the linear transformation taking the ideal element to the physical element; hence $\kappa_w(A) = |S| |S^{-1}| = \kappa(S)$. That is, $\kappa(S)$ is the *condition number of the linear transformation between the ideal and physical tetrahedron*.

Theorem 4.

Let S be derived from a tetrahedron with positive volume. Then $3/\kappa(S)$ is a tetrahedral shape measure.

Proof.

We use the formal definition given in Dompierre, et. al.[5] to prove this assertion. That is, we show that $3/\kappa(S)$ is (1) continuous, (2) invariant to translations and rotations, (3) has values greater than zero and less than or equal to one, (4) has a value of one if and only if the element is ideal, and (5) has a value of zero for degenerate tetrahedra.

First, it is clear that $|S|$ is a continuous function of the coordinates of T_+ , and likewise so is $|S^{-1}|$. Therefore $\kappa(S)$ is a continuous function of the coordinates of any tetrahedron with positive volume.

Second, the Jacobian matrix is invariant to translations so $\kappa(S)$ is invariant to translations. Let $\tilde{A} = \lambda R A$ with $\lambda > 0$ and R a rotation matrix, corresponding to a uniform scaling and rotation of the tetrahedron. Let $\tilde{S} = \tilde{A}W^{-1}$. Because the Frobenius norm is invariant under rotations, it is clear that $\kappa(\tilde{S}) = \kappa(S)$. Finally, $\kappa(S)$ is invariant to scaling because for any real number, ϵ , the definition of condition number directly shows that $\kappa(\epsilon S) = \kappa(S)$.

Third, it is clear that $0 < 3/\kappa(S)$. For any matrix, $|S|^2$ is the sum of the squares of its singular values σ_i . Thus

$$\kappa^2(S) = \sum_{i,j} (\sigma_i/\sigma_j)^2.$$

This is a continuous function of three variables and its minimum may be found by computing the solution to $\partial\kappa^2/\partial\sigma_i = 0$ with $i = 1, 2, 3$. The solution is $\sigma_i = \sigma$ where σ is any positive constant. Hence $\kappa(S) \geq 3$. This shows that $0 < 3/\kappa(S) \leq 1$.

Fourth, suppose $3/\kappa(S) = 1$. Then the singular values of S must be constant and $S = \sigma R$. Then the Jacobian matrix associated with the tetrahedron must have the form $A = \sigma R W$, in other words, $3/\kappa(S)$ attains its maximum value only if the tetrahedral element is a rotation and uniform scaling of the ideal tetrahedron. The converse is easy to show.

Fifth, the definition of a degenerate tetrahedral element given in Dompierre, et. al.[5] is somewhat vague. As noted, a tetrahedron with a small volume is not necessarily degenerate. This is reflected in the properties of the condition number. For example, if $A = \epsilon W$, where $0 < \epsilon \ll 1$, then $\alpha = \epsilon^3 \det(W)$ is small, but $3/\kappa_w(\epsilon W) = 1$. Thus a tetrahedron with small volume does not necessarily make $3/\kappa(S)$ large. Dompierre, et. al. give an example of a degenerate tetrahedron, one whose volume goes to zero but at least some of the lengths do not. Suppose there exist constants b and c such that $0 < b \leq |S|$ and $0 < c \leq |adj(S)|$. Then both $|A|$ and $|adj(A)|$ are bounded below by a positive constant. Because

$$\kappa(S) = |S| |adj(S)| / \det(S),$$

the limit of $3/\kappa(S)$ as $\alpha \rightarrow 0$ is zero. Hence, for the given example, the condition number satisfies the requirement that a shape measure go to zero for a degenerate element. In fact, the condition number provides a rigorous definition of a degenerate element. Let $0 < \epsilon \ll 1$ be given. Then T_+ is degenerate if $3/\kappa(S) < \epsilon$. §

The distinguishing feature between the condition number metric and the other weighted nondimensional quality metrics given in Knupp[15] is given in the following well-known theorem[4] adapted to our current setting.

Theorem 5.

$1/\kappa(S)$ is the greatest lower bound for the distance of S to the set of singular matrices.

Proof.

Let S and X be 3×3 matrices with S non-singular and $S+X$ singular. Write $S+X = S(I+S^{-1}X)$. If $|S^{-1}X| < 1$, then $I+S^{-1}X$ is nonsingular. This would mean that $S+X$ is nonsingular, so we must have $|S^{-1}X| \geq 1$. But $1 \leq |S^{-1}X| \leq |S^{-1}| |X|$; hence $|X|/|S| \geq 1/\kappa(S)$. Therefore

$$\min \{ |X|/|S| : S+X \text{ singular} \} = 1/\kappa(S).$$

§

Because S is singular if and only if A is singular, we are guaranteed that minimization of $\kappa(S)$ will increase the distance between A and the set of singular matrices.

Results similar to those presented in this section can be given for triangular elements.

2.3. The Condition Number of Poor Quality Tetrahedral Elements

The second author reported numerical experiments which show that the common tetrahedral shape degeneracies can be detected by the condition number.[15] We now consider the taxonomy of poorly-shaped tetrahedra given in Cheng, et. al.[3] which is shown in Figure 2. The primary characteristic of these elements is that the four vertices are either nearly linear as shown in the top row or nearly planar as shown in the bottom row.

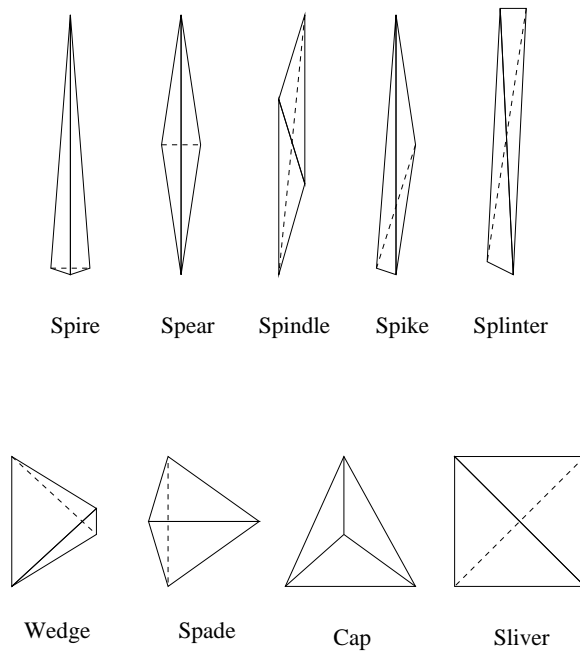


Figure 2. Poor-quality tetrahedral elements

We now examine the behavior of the condition number metric as the quality of each of the nine poorly-shaped tetrahedra worsens. We report the value of the function $\kappa(S)/3$ rather than $3/\kappa(S)$ so that $\kappa(S) = 1$ for an ideal element and $\kappa(S) \rightarrow \infty$ as the element becomes increasingly distorted. We compare this metric to two commonly used quality metrics: minimum dihedral angle and element aspect ratio defined as

$$A_\gamma = \frac{\left(\frac{1}{6} \sum_{i=1}^6 L_i^2\right)^{\frac{3}{2}}}{8.47967\mathcal{V}} \quad (2)$$

where L_i is the length of each edge of the tetrahedron and \mathcal{V} is the volume.[21] The aspect ratio metric is also normalized so that $A_\gamma = 1$ corresponds to an ideal element and $A_\gamma \rightarrow \infty$ as the

element becomes increasingly distorted.

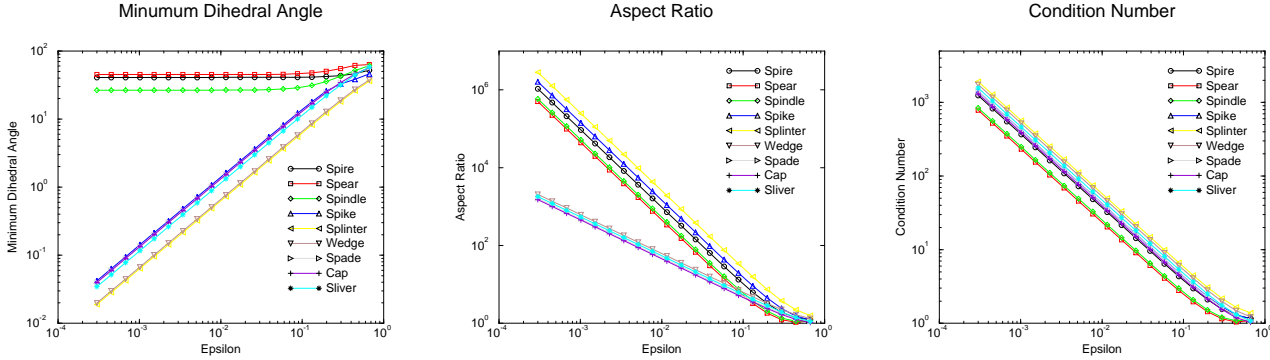


Figure 3. The minimum dihedral angle, aspect ratio, and condition number metrics as a function of tetrahedral element quality

For each element type shown in Figure 2, we create a series of poor quality tetrahedra and compute and plot the resulting metric values in the log-log graphs shown in Figure 3. We start with the ideal tetrahedral element and modify it so that the vertices are no more than a distance of ϵ from the center line for the elements in the first row and are no taller than ϵ for the element types in the second row. In Figure 3 we plot the values for each of the metric as ϵ decreases. Ideally, the minimum dihedral angle should decrease as the tetrahedra become increasingly distorted. However, this metric is not a tetrahedral shape measure as defined by Dompierre et. al.[5] which is reflected by the fact that it is unable to detect spear, spindle, or spire elements. In contrast, both the aspect ratio and condition number metrics effectively detect all nine distorted element types. In addition, the dihedral angle metric is more expensive to compute than the other two because there are six values per tetrahedron rather than one. In particular, on a Sun Ultra 2 with 300 MHz processors, the dihedral angle metric required $1.73 \cdot 10^{-4}$ seconds to compute for each tetrahedron, whereas the the aspect ratio and condition number metrics required $3.80 \cdot 10^{-5}$ and $6.58 \cdot 10^{-5}$ seconds, respectively.

3. Optimization-based Smoothing Techniques

Using the element condition number quality metric, we now derive two objective functions that are useful for optimization-based mesh improvement. We then briefly describe the associated optimization algorithms; more details can be found in the references mentioned below.

3.1. Optimization Objective Functions

To build objective functions for mesh improvement based on the condition number of the tetrahedron, consider a node in the interior of a valid tetrahedral mesh with M attached tetrahedra. Let A_m be a Jacobian matrix corresponding to the m th element and $S_m = A_m W^{-1}$. Let $\kappa_m = \kappa(S_m)$, $m = 0, 1, \dots, M-1$, be the weighted condition number of the m th attached tetrahedron normalized so that an equilateral tetrahedron has a κ value of one, and $K = (\kappa_0, \kappa_1, \dots, \kappa_{M-1})$. The vector

p -norm of K can be used to construct a local objective function to minimize the condition number

$$\|K\|_p = \left[\sum_{m=0}^{M-1} \kappa_m^p \right]^{1/p}.$$

The choice $p = 2$ gives the ℓ_2 norm of K

$$\|K\|_2 = \left[\sum_{m=0}^{M-1} \kappa_m^2 \right]^{1/2}, \quad (3)$$

which can be used to minimize the average condition number, while $p \rightarrow \infty$ gives the ℓ_∞ norm

$$\|K\|_\infty = \max_m \{\kappa_m\},$$

which can be used to minimize the maximum condition number. For the results presented in Section 4, we reformulate the objective function as the equivalent maximization problem as follows:

$$K_{min} = \min_m \{-\kappa_m\}. \quad (4)$$

Because the condition number is not defined for elements with negative volume, one must begin optimization with a valid mesh. To achieve this, the mesh is pre-processed with an untangling objective function based on the ℓ_∞ norm of the Jacobian determinant.[12, 10, 18] We note that some optimization techniques require the gradient of the condition number $\kappa(S)$ with respect to the free vertex position \mathbf{x} . Let $S = AW^{-1}$. One can apply the chain rule and the formulas given in Knupp[15] to compactly write the gradient:

$$\nabla \kappa = -\frac{\partial \kappa}{\partial S} W^{-T} u$$

with $u^T = [1, 1, 1]$. An explicit calculation shows that

$$\frac{\partial \kappa}{\partial S} = \frac{\|S\|^2 S}{\det(S)^2 \kappa(S)} \left[\|S\|^2 I - S^T S \right] - \kappa(S) S^{-T} + \|S^{-1}\|^2 \frac{S}{\kappa(S)}.$$

3.2. Optimization Procedures

We now formulate the optimization problem associated with each of the objective functions given above. In each case, the characteristics of the objective function demand different solution techniques, and we briefly describe the methods used.

Optimization of the ℓ_2 objective function. The formulation of the optimization problem for the ℓ_2 objective function given in (3) is

$$\min \left[\sum_{m=0}^{M-1} \kappa_m(\mathbf{x})^2 \right]^{1/2}.$$

This objective function is smooth with continuous derivatives, and the problem can be solved with various techniques for unconstrained optimization.

We use a robust minimization algorithm that requires only objective function values. M search directions are computed from the sum of $e_{n+1,n}$ for each of the attached tetrahedra. The objective

function is then evaluated at various distances along the scaled search directions, and the node is moved to the position that provides the greatest decrease in the value of the objective function. If no decrease is found, the node is not moved. See Knupp and Freitag[10] and Knupp[15] for more details.

Optimization of the ℓ_{inf} objective function. The optimization problem for the ℓ_{inf} objective function given in (4) is formulated as

$$\max \min_{0 \leq m \leq M-1} \{-\kappa_m(\mathbf{x})\},$$

where each κ_m is a nonlinear, smooth, and continuously differentiable function of the free vertex position. Let the maximum value of the functions evaluated at \mathbf{x} be called the *active value*, and the set of functions that obtain that value, the *active set*, be denoted by $\mathcal{S}(\mathbf{x})$. Because multiple elements can obtain the maximum value, the composite objective function has discontinuous partial derivatives where the active set changes from one set of functions to another set.

We solve this nonsmooth optimization problem using an analogue of the steepest descent method for smooth functions. The search direction, \mathbf{s} , at each step is the steepest descent direction derived from all possible convex linear combinations of the gradients in $\mathcal{S}(\mathbf{x})$. The line search subproblem along \mathbf{s} is solved by predicting the points at which the active set \mathcal{S} will change. These points are found by computing the intersection of the projection of a current active function in the search direction with the linear approximation of each $-\kappa_m(\mathbf{x})$ given by the first-order Taylor series approximation. The distance to the nearest intersection point from the current location gives the initial step length, β . The initial step is accepted if the actual improvement achieved by moving v exceeds 90 percent of the estimated improvement or the subsequent step results in a smaller function improvement. Otherwise, β is halved recursively until a step is accepted, or β falls below some minimum step length tolerance. More detail on this optimization algorithm can be found in Freitag, et. al.[13] and Freitag[8].

4. Numerical Experiments

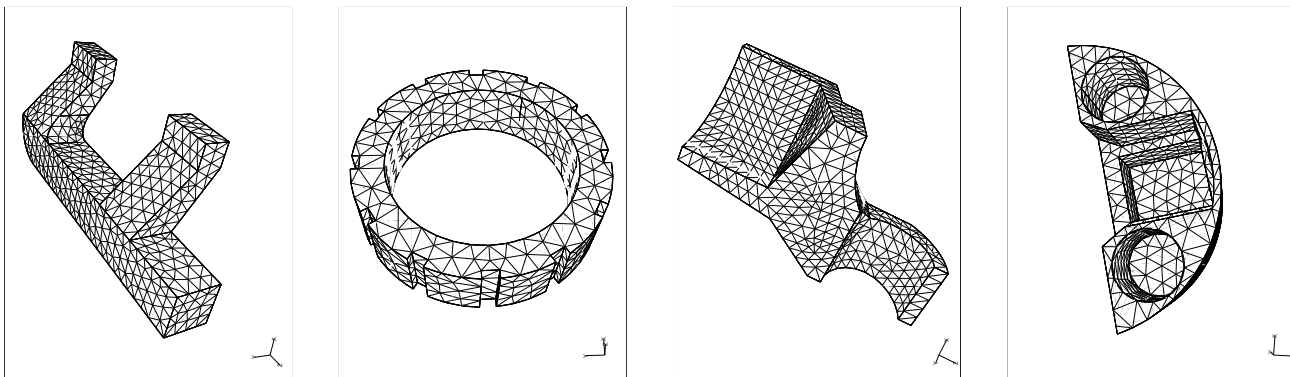


Figure 4. The four tetrahedral mesh test cases for duct, gear, hook and foam geometries

We now demonstrate the effectiveness of each of the optimization techniques in improving tetrahedral meshes compared with a baseline Laplacian smoother. We use four tetrahedral meshes

generated by the CUBIT package[6] for duct, gear, hook, and foam geometries. These meshes are shown in Figure 4. In Table I, we give the number of elements in each mesh, N , and the initial mesh quality as measured by the following metrics:

1. The number of distorted elements in the mesh, N_D , namely those with a normalized condition number greater than 3.0.
2. The average normalized condition number for all of the elements in the mesh, κ_{avg} .
3. The maximum normalized condition number of any element in the mesh, κ_{max} .
4. The average and maximum tetrahedral aspect ratio given by Equation 2.

The overall quality of each initial mesh as measured by κ_{avg} and $A_{\gamma_{avg}}$ is quite good, but each mesh contains a number of distorted elements.

Table I. Initial quality of the four test cases

Geom.	N	N_D	κ_{avg}	κ_{max}	$A_{\gamma_{avg}}$	$A_{\gamma_{max}}$
Duct	4267	39	1.305	3.790	1.441	5.191
Gear	3116	25	1.423	3.448	1.622	4.782
Hook	4675	30	1.360	5.176	1.533	6.151
Foam	4847	47	1.392	4.362	1.579	8.197

Mesh improvement results are obtained by using the CUBIT and Opt-MS[9] software packages developed at Sandia National Laboratories and Argonne National Laboratory, respectively. An interface between these two packages has been developed, and we also report the results of a combined optimization approach that uses the two software packages in concert. We will measure the success of our smoothing techniques by their ability to eliminate distorted elements and to improve both the average and the maximum quality metric values.

We attempt to improve each initial mesh described in Table I with six different smoothing techniques:

1. Laplacian smoothing;
2. “smart” Laplacian smoothing, which accepts a Laplacian step only if the local submesh is improved as measured by κ_{max} ;
3. ℓ_2 smoothing as described in Section 3;
4. ℓ_{inf} smoothing as described in Section 3;
5. restricted ℓ_{inf} smoothing that is applied only if $\kappa_{max} > 3.0$ in the local submesh; and
6. a combined optimization-based approach that uses ℓ_2 smoothing on each local submesh followed by the restricted ℓ_{inf} approach.

In each case, we iterate over the interior nodes in the mesh until the change in all node point positions is smaller than some tolerance.

In Table II we report the results of each technique in terms of the number of distorted elements remaining in the mesh after smoothing, the values of the quality metrics, $q_i = \kappa_{avg}, \kappa_{max}, A_{\gamma_{avg}}, A_{\gamma_{max}}$, as well as the percentage change from the initial value as computed by the formula

$$\mathcal{P}_i = \frac{q_{i\text{final}} - q_{i\text{initial}}}{q_{i\text{initial}}} \times 100.$$

Because of the way the metrics are normalized, a negative \mathcal{P}_i value indicates an improvement in mesh quality whereas a positive \mathcal{P}_i value indicates a worsening of mesh quality. We also report the number of nodes moved during the mesh smoothing process, C_S , which corresponds to the number of calls made to each smoother. For the combined approach, C_S is reported as the number of calls to the ℓ_2 smoother, C_1 , plus the number of calls to the ℓ_{inf} smoother, C_2 , and is denoted (C_1, C_2) .

Table II. Mesh quality improvement results for the optimization-based smoothing techniques

Technique	N_D (\mathcal{P})	κ_{avg} (\mathcal{P})	κ_{max} (\mathcal{P})	$A_{\gamma_{avg}}$ (\mathcal{P})	$A_{\gamma_{max}}$ (\mathcal{P})	C_S
Duct Geometry						
Laplacian	78 (+100)	–	–	1.452 (+.76)	24.25 (+367)	1303
Smart Lap.	31 (-20.5)	1.300 (-.38)	3.691 (-2.6)	1.433 (-.56)	4.964 (4.3)	732
ℓ_2 Opt.	15 (-62)	1.275 (-2.2)	3.690 (-2.6)	1.400 (-2.8)	4.578 (-11.8)	2773
ℓ_{inf} Opt.	4 (-90)	1.379 (+5.7)	3.045 (-19.7)	1.571 (+9.0)	3.979 (-23.3)	5498
Restricted ℓ_{inf}	4 (-90)	1.313 (+.61)	3.045 (-19.7)	1.493 (+3.6)	3.979 (-23.3)	32
Combined	4 (-90)	1.280 (-2.2)	3.045 (-19.7)	1.409 (-2.2)	3.980 (-23.3)	(2773,13)
Gear Geometry						
Laplacian	63 (+152)	–	–	1.661 (+2.4)	84.80 (+1673)	1051
Smart Lap.	11 (-56)	1.414 (-.63)	3.309 (-4.0)	1.610 (-.74)	4.782 (0)	492
ℓ_2 Opt.	3 (-88)	1.378 (-3.2)	3.657 (+6.1)	1.560 (-3.8)	5.201 (+8.8)	2141
ℓ_{inf} Opt.	0 (-100)	1.455 (+2.2)	2.996 (-13.1)	1.682 (+3.6)	3.703 (-22.5)	2213
Restricted ℓ_{inf}	0 (-100)	1.425 (+.14)	2.996 (-13.1)	1.627 (+.31)	4.744 (-13.1)	24
Combined	0 (-100)	1.380 (-3.0)	2.996 (-13.1)	1.562 (-3.6)	3.953 (-17.3)	(2141,3)
Hook Geometry						
Laplacian	64 (+113)	1.393 (+2.4)	74.28 (+1335)	1.569 (+2.3)	88.19 (+1334)	1443
Smart Lap.	27 (-10)	1.356 (-.25)	5.176 (0)	1.529 (-.26)	6.151 (0)	798
ℓ_2 Opt.	7 (-77)	1.331 (-2.1)	3.747 (-27.6)	1.495 (-2.4)	4.437 (-27.9)	2933
ℓ_{inf} Opt.	0 (-100)	1.429 (+5.1)	2.973 (-48.0)	1.659 (+8.2)	4.331 (-29.6)	5970
Restricted ℓ_{inf}	0 (-100)	1.367 (+.51)	2.990 (-42.2)	1.549 (+1.0)	4.331 (-29.6)	34
Combined	0 (-100)	1.332 (-2.1)	2.973 (-42.6)	1.497 (-2.3)	4.331 (-29.6)	(2933,5)
Foam Geometry						
Laplacian	82 (+74)	–	–	1.622 (+2.7)	83.17 (+914)	916
Smart Lap.	42 (-11)	1.390 (-.14)	4.362 (0)	1.575 (-.25)	8.197 (0)	555
ℓ_2 Opt.	21 (-55)	1.372 (-1.4)	4.310 (-1.2)	1.552 (-1.7)	6.760 (-17.5)	2637
ℓ_{inf} Opt.	25 (-47)	1.447 (+4.0)	4.310 (-1.2)	1.672 (+5.8)	6.596 (-19.5)	3376
Restricted ℓ_{inf}	25 (-53)	1.398 (+.43)	4.310 (-1.2)	1.590 (+.70)	6.596 (-19.5)	33
Combined	24 (-49)	1.375 (-1.2)	4.310 (-1.2)	1.556 (-1.4)	6.596 (-19.5)	(2637,11)

In three of the four cases, Laplacian smoothing results in a mesh containing inverted elements. The CUBIT software defines the condition number of inverted elements to be 10^6 , which skews the κ_{avg} and κ_{max} values for those meshes; we do not report those results. In all four cases, Laplacian smoothing worsens mesh quality by every measure reported: the number of distorted elements is approximately doubled, $A_{\gamma_{avg}}$ increases by more than two percent, and $A_{\gamma_{max}}$ is significantly worsened in all four cases. By design, the “smart” Laplacian smoother improves the mesh in each

case, but the improvement in the average element quality is less than .5 percent in all cases, and the improvement in the maximum quality values is zero in two of the four cases.

In contrast, the optimization-based smoothing approaches preserve mesh validity in all four test cases, and each approach significantly improves the mesh by some measure of mesh quality. Both the ℓ_2 and ℓ_{inf} smoothers are able to eliminate a majority of the distorted elements. The ℓ_{inf} smoother typically does better than ℓ_2 with respect to this metric, and in two of the four cases eliminates all of the distorted elements from the mesh. As expected, the ℓ_2 smoother improves the average element quality in all four cases by as much 3.2 percent. Although it is not designed to improve κ_{max} , this can happen serendipitously as is evidenced in three of the four cases. In the gear geometry, however, κ_{max} worsens by about 6 percent. The results for the ℓ_{inf} smoother are the inverse of the ℓ_2 results. The average element quality is worsened in each case by as much as 5.7 percent in the duct geometry, but the κ_{max} and $A_{\gamma_{max}}$ values are always significantly improved. The restricted ℓ_{inf} smoother achieves nearly the same improvement in κ_{max} and $A_{\gamma_{max}}$ as the ℓ_{inf} smoother without the corresponding decrease in average element quality and at a significantly smaller cost. The combined optimization approach achieves the best overall improvement in each of the four cases; all quality metrics are significantly improved in all test cases, and its use is recommended.

In each case the number of calls to the ℓ_2 smoother is roughly equal to the number of vertices in the mesh. In contrast the ℓ_{inf} smoother is called more times, indicating more grid point movement. This is supported by the fact that the average element quality changes approximately twice as much when the ℓ_{inf} smoother is called significantly more times than the ℓ_2 smoother. The restricted ℓ_{inf} smoother is called approximately once for each distorted element in the mesh when used alone, and far fewer times when used in conjunction with the ℓ_2 smoother. Currently the ℓ_{inf} and ℓ_2 smoothers are about ten and one hundred times more expensive than smart Laplacian, respectively, and work to reduce computational cost is under way.

5. Conclusions

Our results indicate that Laplacian smoothing can be detrimental to the quality of simplicial meshes on complex geometries, and we do not recommend its use. In contrast, the optimization approaches, particularly the combined ℓ_2 and ℓ_{inf} smoothing technique, significantly improved the quality of each of the test cases. We showed that the behavior of the more commonly accepted aspect ratio shape measure was mirrored by the behavior of the condition number shape measure, and that the condition number shape measure is theoretically optimal. In addition, the fact that the condition number metric can be referenced to any ideal element through the use of the weighting matrix makes it far more flexible than its geometric counterparts.

Strategically combining different local mesh smoothing strategies is not a new idea; a number of researchers have combined Laplacian smoothing with their optimization-based approaches to achieve good quality meshes at a low computational cost.[23, 8] However, this is the first instance we are aware of in which two optimization strategies have been combined to improve both the average element quality and the extremal element quality. Although our results showed that these improvements can be achieved for a small incremental cost to the ℓ_2 strategy, further work is needed to reduce the overall cost of the approach. Techniques that combine Laplacian smoothing with the combined technique presented here are under consideration.

Finally, we note that the algorithms presented in this paper for smoothing and untangling are local techniques; a globally optimal solution is not guaranteed although empirical evidence suggests

that the techniques work well in practice.

REFERENCES

1. R. E. Bank and R. K. Smith. Mesh smoothing using a posteriori error estimates. *SIAM Journal on Numerical Analysis*, 34(3):979–997, June 1997.
2. Randy Bank. *PLTMG: A Software Package for Solving Elliptic Parital Differential Equations, Users' Guide 7.0*, volume 15 of *Frontiers in Applied Mathematics*. SIAM, Philadelphia, 1994.
3. Siu-Wing Cheng, Tamal Dey, Herbert Edelsbrunner, Michael Facello, and Shang-Hua Teng. Sliver exudation. In *ACM Symposium on Computational Geometry*, pages 1–13. 1999.
4. J. Demmel. *Applied Numerical Linear Algebra*. SIAM, Philadelphia, Pennsylvania, 1997.
5. J. Dompierre, P. Labbe, F. Guibault, and R. Camerero. Proposal of benchmarks for 3d unstructured tetrahedral mesh optimization. In *Proceedings of the 7th International Meshing RoundTable'98*, pages 459–478, 1998.
6. T. D. Blacker et. al. CUBIT mesh generation environment. Technical Report SAND94-1100, Sandia National Laboratories, Albuquerque, New Mexico, May 1994.
7. David A. Field. Laplacian smoothing and Delaunay triangulations. *Communications and Applied Numerical Methods*, 4:709–712, 1988.
8. Lori Freitag. On combining Laplacian and optimization-based smoothing techniques. In *Trends in Unstructured Mesh Generation*, volume AMD-Vol. 220, pages 37–44. ASME Applied Mechanics Division, 1997.
9. Lori Freitag. Users manual for Opt-MS: Local methods for simplicial mesh smoothing and untangling. Technical Report ANL/MCS-TM-239, Mathematics and Computer Science Division, Argonne National Laboratory, Argonne, Ill., 1999.
10. Lori Freitag and Patrick Knupp. Tetrahedral element shape optimization via the jacobian determinant and condition number. In *Proceedings of the Eighth International Meshing Roundtable*, pages 247–258. Sandia National Laboratories, 1999.
11. Lori Freitag and Carl Ollivier-Gooch. A comparison of tetrahedral mesh improvement techniques. In *Proceedings of the Fifth International Meshing Roundtable*, pages 87–100. Sandia National Laboratories, 1996.
12. Lori Freitag and Paul Plassmann. Local optimization-based simplicial mesh untangling and improvement. Preprint ANL/MCS-P749-0399, Mathematics and Computer Science Division, Argonne National Laboratory, Argonne, Ill., August, 1999.
13. Lori A. Freitag, Mark T. Jones, and Paul E. Plassmann. An efficient parallel algorithm for mesh smoothing. In *Proceedings of the Fourth International Meshing Roundtable*, pages 47–58. Sandia National Laboratories, 1995.
14. P. L. George and H. Borouchaki. *Delaunay Triangulation and Meshing*. Hermes, Paris, 1998.
15. Patrick Knupp. Achieving finite element mesh quality via optimization of the Jacobian matrix norm and associated quantities, Part II - A framework for volume mesh optimization. Technical Report SAND 99-0709J, Sandia National Laboratories, 1999.
16. Patrick Knupp. Achieving finite element mesh quality via optimization of the Jacobian matrix norm and associated quantities, Part I - A framework for surface mesh optimization. *International Journal of Numerical Methods in Engineering*, 48(3):401–420, 2000.
17. Patrick Knupp. Algebraic mesh quality metrics. Technical Report SAND 00-, Sandia National Laboratories, 2000.
18. Patrick Knupp. Non-simplicial mesh untangling. Technical Report SAND 00-, Sandia National Laboratories, 2000.
19. A. Liu and B. Joe. Relationship between tetrahedron quality measures. *BIT*, 34:268–287, 1994.
20. S. H. Lo. A new mesh generation scheme for arbitrary planar domains. *International Journal for Numerical Methods in Engineering*, 21:1403–1426, 1985.
21. V. N. Parthasarathy, C. M. Graichen, and A. F. Hathaway. A comparison of tetrahedron quality measures. *Finite Element Analysis and Design*, 15:255–261, 1993.
22. Matthew L. Staten Scott A. Canann, Joseph R. Tristano. An approach to combined Laplacian and optimization-based smoothing for triangular, quadrilateral, and quad-dominant meshes. In *Proceedings of the 7th International Meshing Roundtable*, pages 479–494. Sandia National Laboratories, 1998.
23. Mark Shephard and Marcel Georges. Automatic three-dimensional mesh generation by the finite octree technique. *International Journal for Numerical Methods in Engineering*, 32:709–749, 1991.